Chemistry and Materials

The Center for Science Innovation

Research Article

Chem. Mater. 4 (1) 2025, 34-42

PtSnNi Trimetallic and Their Catalytic Activities in Ethanol Electrooxidation

Hilman Syafei[1,*], **Raudhatul Hadawiyah**[2], **Mulya Muhammad Nur**[3]

[1]Department of Physic, Faculty of Mathematics and Naturals Sciences, Universitas Indonesia, Kampus UI Depok, Depok 16424, Indonesia

[2]The Center for Science Innovation, No. 40 BC Arva Building, Jl. RP. Soeroso, Jakarta Pusat 10350, Indonesia

[3]Department of Chemistry, King Fahd University of Petroleum & Minerals, Dhahran, 31261, Saudi Arabia

*Corresponding author: hilman.syafei@ui.ac.id

Received
9 January 2025
Received in revised form
4 February 2025
Accepted
25 February 2025
Published online
28 February 2025
DOI
https://doi.org/10.56425/cma.v4i1.90

Abstract

The declining availability of fossil fuels and their environmental impacts have driven the search for cleaner, renewable energy alternatives, such as direct ethanol fuel cells (DEFCs). However, the widespread application of DEFCs faces challenges due to the complex kinetics of ethanol electrooxidation, necessitating the development of effective catalysts. Platinum (Pt) is widely regarded as the most effective catalyst for this process. However, its use is hindered by high costs and susceptibility to poisoning by intermediates formed during the ethanol electrooxidation reaction. To address these issues, the addition of Sn and Ni to the Pt catalyst is expected to enhance its performance. In this study, PtSnNi trimetallics were synthesized using the electrodeposition method. The samples were then characterized using scanning electron microscopy-energy dispersive spectroscopy (SEM-EDX) and electrochemical tests to evaluate their catalytic activity and stability. The SEM image reveals that PtSnNi2 has the smallest particle size compared to other PtSnNi samples. Additionally, the results indicate that PtSnNi2, with a composition of 73% Pt, 26% Sn, and 1% Ni, exhibits the optimal electrolyte concentration, leading to the highest catalytic activity and stability. This is evidenced by the lowest R_{ct}, lowest I_b/I_f ratio, and highest current density in the ethanol oxidation reaction.

Keywords: PtSnNi trimetallic, ethanol electrooxidation, chemical composition

1. Introduction

Conventional fuels, derived from fossil resources or coal and used daily, are becoming increasingly scarce and may eventually be depleted. In addition to their scarcity, these fuels significantly contribute to climate change and greenhouse gas emissions, posing serious environmental challenges [1,2]. The reliance on conventional fuels can be addressed by transitioning to renewable fuels, which also help reduce carbon emissions. One promising alternative is ethanol fuel, often utilized in direct ethanol fuel cells (DEFCs) [3–6]. DEFCs have been extensively studied as a replacement for conventional fuels and as an alternative to other energy sources like hydrogen [7–9] and methanol [10,11]. Ethanol, a type of alcohol, is advantageous because it can be easily produced through the fermentation of biomass, yielding large quantities [12–15]. Additionally, ethanol offers higher energy output compared to hydrogen and methanol due to its two C-C bonds, which provide significant energy yields while maintaining lower toxicity [3].

DEFCs offer numerous environmental benefits, but they require serious attention due to challenges associated with breaking the C-C bonds during ethanol oxidation reaction (EOR) [16]. This process demands high activation energy and is hindered by the formation of intermediates, which pose significant obstacles to DEFC development. Consequently, enhancing DEFC performance necessitates a focused effort on optimizing the catalysts used in the EOR process [17].

Catalysts play a crucial role in enhancing catalytic activity during the EOR process. Various metals, including Pt [18], Pd [19], Co [20], Ni [21], Au [22], Cu [23], and others, have been extensively studied for their effectiveness in DEFC systems. Noble metals like Pt have demonstrated excellent catalytic activity. However, their performance tends to decrease as the EOR process progresses. This is primarily due to the inhibition of active sites caused by CO adsorption as an intermediate phase [24,25]. Additionally, the high cost of Pt presents another challenge in its widespread use. To address these issues, combining Pt with other metals to form bimetallic or trimetallic catalysts is a promising approach to improve its performance while potentially reducing costs [26,27].

Enhancing catalyst performance to a trimetallic composition for the EOR process offers a promising solution to the limitations of Pt-based catalysts. Incorporating metals that are more abundant in nature, such as Co [28], Sn [29], and Ni [30], has drawn significant attention due to their potential to improve catalytic performance. Sn and Ni are oxophilic metals, meaning they facilitate the dissociation of water into OH^-, which is essential for oxidizing intermediates during the EOR process [25].

Sun et al. [31] demonstrated that $Pt_{73}Sn_{27}$ exhibits higher activity and stability during the EOR process compared to commercial Pt/C catalysts. Similarly, Luo et al. [32] reported that a PtNi trimetallic with a Pt:Ni ratio of 1.7 showed enhanced catalytic activity. Further research by Mauer et al. [33] revealed that PtSnNi, as a trimetallic catalyst, not only outperforms commercial Pt/C but also surpasses bimetallic with various compositions, making it a compelling candidate for EOR applications. This research can be further expanded to investigate the composition of PtSnNi trimetallic catalysts to determine the optimal ratio for enhancing EOR performance. The composition of Pt and Sn will be adjusted, as variations in their proportions may lead to different EOR outcomes [34,35]

In this study, the composition of the PtSnNi catalysts were investigated using the electrodeposition method. This technique is a quick and straightforward approach for manipulating the sample size and morphology [36]. The research was focused on combining Pt, Sn, and Ni electrolyte solutions to determine the optimum composition of PtSnNi for the EOR process, with an emphasis on maximizing catalytic activity and stability.

2. Materials and Method

2.1 Materials

PtSnNi is synthesized with metal precursors K_2PtCl_6 (99% purity, sigma-aldrich), $SnCl_2$ (98% purity, sigma-aldrich), $NiSO_4 \cdot 6H_2O$ (99% purity, sigma-aldrich). The solvent used through electrodeposition is H_2SO_4 (96% purity, Sigma-Aldrich), and HCl (37%, Merck). Electrochemical characterization in the EIS process used KCl (98% purity, Merck), while the EOR process used ethanol (98% purity, Merck) and NaOH (Merck). For substrate, Cu (1.5 cm, diameter 0.5 cm) is used. All the distilled water used in this research is high-purity water.

2.2 Methods

2.2.1 Synthesize of PtSnNi

The Cu substrate was ultrasonicated for 10 minutes in distilled water, then cleaned and dried. The PtSnNi solution was prepared under the following conditions: (i) K_2PtCl_6 and $NiSO_4 \cdot 6H_2O$ were dissolved in 5 mL of H_2SO_4, and (ii) $SnCl_2$ was dissolved in 10 mL of HCl. The solution was then varied into several concentrations, as shown in Table 1.

The solution was placed into the chamber for the synthesis process. Synthesis was conducted at a voltage of -1.5 V for 10 minutes. The synthesized material was subsequently cleaned and prepared for characterization and electrochemical testing.

Table 1. Concentration of Pt, Sn, and Ni of each sample.

Sample	Concentration (M)		
	Pt	Sn	Ni
PtSnNi1	0.001	0.009	0.02
PtSnNi2	0.0025	0.0075	0.02
PtSnNi3	0.005	0.005	0.02
PtSnNi4	0.0075	0.0025	0.02

2.2.2 Characterization

The PtSnNi trimetallic sample was characterized using scanning electron microscopy with energy-dispersive X-ray spectroscopy (SEM-EDX) to analyze the morphology and composition of PtSnNi.

2.2.3 Electrochemical tests

PtSnNi samples were evaluated for their catalytic activity and stability. The first test, electrochemical impedance spectroscopy (EIS), was conducted to measure the impedance of the samples. Linear sweep voltammetry (LSV) was performed to assess the reaction kinetics through the Tafel slope. The EOR test was carried out using the cyclic voltammetry (CV) method with a solution of 1.0 M ethanol and 1.0 M NaOH (25 mL) for 1000 cycles to evaluate the stability.

3. Results and Discussion

Figure 1 shows the XRD diffraction pattern of PtSnNi. The peak at 38.11° corresponds to Pt with the (111) plane, confirming its face-centered cubic (FCC) structure [18,37]. Additionally, peaks at approximately 43°, 51°, 74°, 90°, and 95° are attributed to the copper substrate, as referenced in COD ID 7101269. The PtSnNi phase is not clearly visible in the XRD characterization due to the small size and rod-like shape of the substrate.

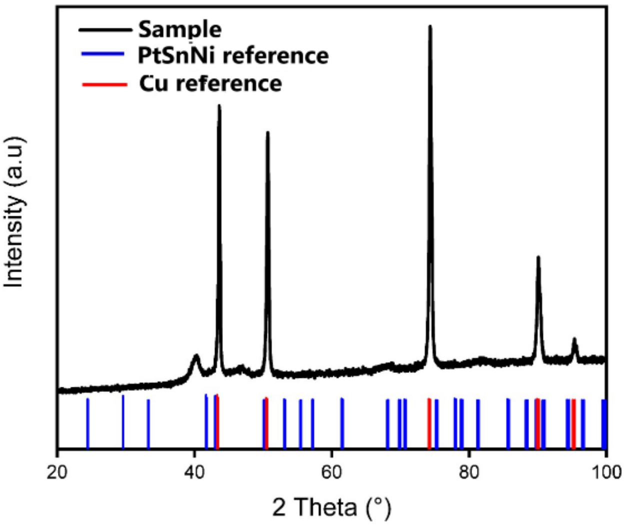

Figure 1. XRD pattern of PtSnNi/Cu.

Figure 2 presents micrographs of PtSnNi samples synthesized with varying solution compositions. The corresponding compositional data are provided in Table 2. The PtSnNi samples generally exhibit a spherical morphology. However, notable differences in particle distribution are observed among the samples. For PtSnNi1, PtSnNi3, and PtSnNi4, the particles tend to cluster at specific sites and exhibit relatively large sizes. In contrast, PtSnNi2 displays a more uniform particle distribution across the substrate.

Table 2. Composition of Pt, Sn, and Ni in all sample.

Sample	Composition (wt%)		
	Pt	Sn	Ni
PtSnNi1	13%	77%	10%
PtSnNi2	73%	26%	1%
PtSnNi3	90%	8%	2%
PtSnNi4	93%	4%	3%

The composition of PtSnNi is strongly influenced by the concentrations of precursors. In the progression from PtSnNi1 to PtSnNi4, the concentration of Pt increases, while that of Sn decreases. This trend is reflected in the corresponding increase in the Pt percentage in the samples. Pt^{2+} ions have a lower reduction potential compared to Sn and Ni ions, resulting in a significantly higher deposition of Pt [38,39]. Additionally, Pt has higher electronegativity compared to Sn and Ni enhances its tendency to attract electrons, leading to a higher electron density around the Pt atoms. This difference in electronegativity causes external electrons from Sn and Ni atoms to be drawn towards Pt, effectively reducing the concentration of Sn and Ni in the trimetallic [40].

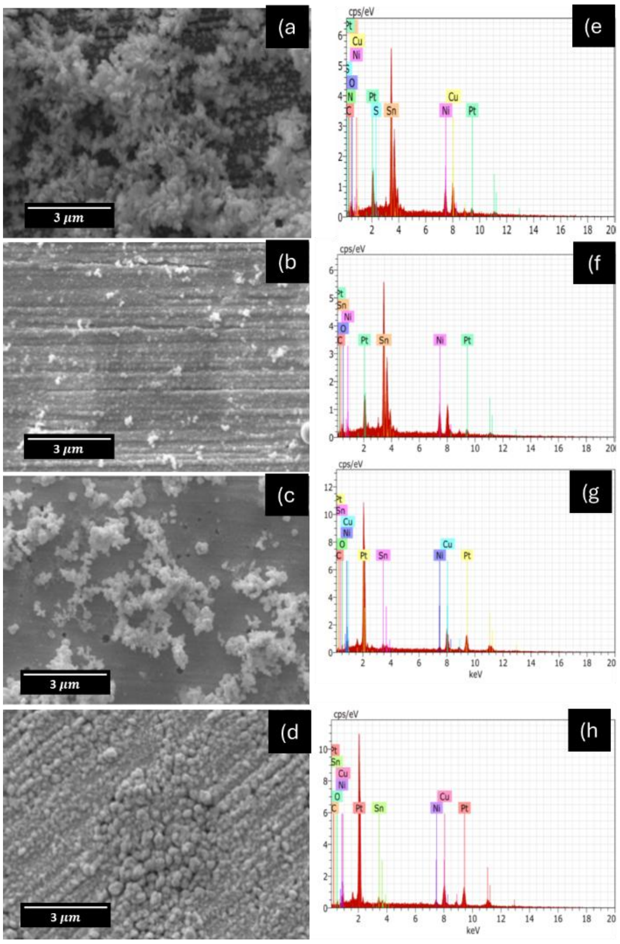

Figure 2. SEM images and EDX point analysis of PtSnNi samples: (a,e) PtSnNi1, (b,f) PtSnNi2, (c,g) PtSnNi3, and (d,h) PtSnNi4.

Figure 5 presents the EOR results of the PtSnNi displayed as voltammogram graphs. An anodic peak is observed in all catalysts, confirming that the electrooxidation of ethanol occurs in alkaline media [43]. Two distinct peaks are present in each curve, corresponding to the forward and backward scans.

The forward scan peak appears at potentials ranging from -0.1 V to 0.4 V, while the backward scan peak is observed between -0.3 V and -0.1 V. The pronounced peak in the forward scan is attributed to the oxidation of chemical species resulting from the adsorption of ethanol onto the catalyst surface. In contrast, the backward scan peak corresponds to the removal of intermediate substances that were not fully oxidized during the forward scan [44].

The precursor concentrations and solution composition also play a critical role in the particle growth process. The use of H_2SO_4 in the synthesis promotes the conductivity and reduction of Pt and Ni, while HCl stabilizes Sn ions, reducing the extent of Sn reduction. Consequently, a lower concentration of HCl decreases the Sn content in the trimetallic, while increasing the Pt precursor concentration leads to a higher Pt content.

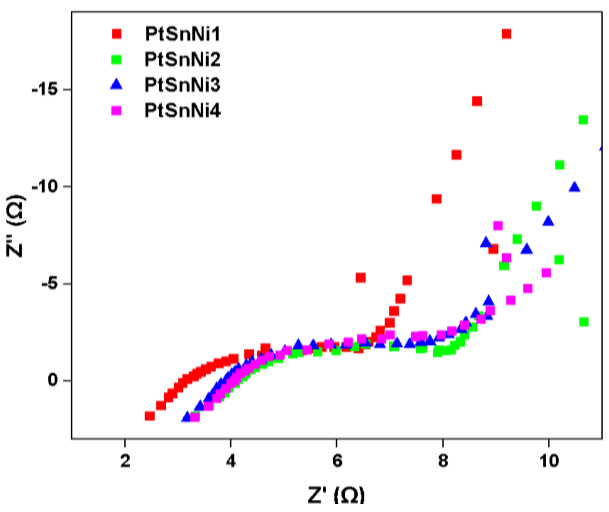

Figure 3. Nyquist plot of PtSnNi with different composition.

Figure 3 presents the Nyquist plots for all PtSnNi samples. Each plot exhibits a semicircle, indicative of charge transfer resistance (R_{ct}). The R_{ct} values are summarized in Table 3. Among the samples, PtSnNi2 demonstrates the lowest R_{ct}, consistent with the SEM characterization. A lower R_{ct} value indicates a faster reaction rate. This is attributed to its superior morphology, uniform particle distribution, and smaller particle size compared to the other PtSnNi samples. Additionally, the elemental composition significantly influences R_{ct} due to the synergistic effect of Sn and Ni in facilitating the removal of intermediate species.

Table 3. R_{ct} of the various synthesized PtSnNi alloy catalysts determined from the recorded Nyquist Plot.

Sample	R_{ct} (Ω)
PtSnNi1	3.636
PtSnNi2	2.040
PtSnNi3	3.099
PtSnNi4	3.450

Figure 4 shows LSV curves obtained using ethanol and NaOH solutions to evaluate the catalytic activity of the catalysts. The results produce a Tafel slope graph, as shown in Fig. 4b. The Tafel slope is used to analyze the rate and mechanism of electrocatalytic reactions, representing the number of millivolts (mV) required to increase the current by a factor of 10, expressed in mV/dec [41]. The Tafel slope values for the PtSnNi1, PtSnNi2, PtSnNi3, and PtSnNi4 catalysts are 88 mV/dec, 158.67 mV/dec, 113.7 mV/and 64.61 mV/dec, respectively. A lower Tafel slope value indicates faster reaction kinetics, as a smaller overpotential is required to achieve higher current densities [41,42].

PtSnNi4 exhibits the lowest Tafel slope, attributed to its high Pt content, as confirmed by EDX composition analysis, providing the most active sites for the reaction and resulting in the highest reaction kinetics. Similarly, PtSnNi3, which has a high Sn content, also shows rapid reaction rates due to the efficient oxidation of intermediates facilitated by Sn. In contrast, PtSnNi2, with a composition of 73 wt.% Pt, has the highest Tafel slope value. This is because the active Pt sites are balanced with Sn active sites, which primarily oxidize intermediate species that do not directly contribute to ethanol oxidation. This balancing limit the ability of the catalyst to sustain fast kinetics, resulting in a higher Tafel slope.

Figure 5 also compares the performance of each PtSnNi catalyst at its highest cycle, highlighting the differences in catalytic activity among the samples. The PtSnNi2 catalyst has the highest current density, namely 117.25 mA/cm^2, indicating that this catalyst can produce a greater current during ethanol electrooxidation compared to other compositions. A low I_b/I_f ratio is also shown by the PtSnNi2 catalyst, namely 0.1508, which indicates that this catalyst has an efficient ability to oxidize intermediate products such as CO [45]. With a low I_b/I_f ratio, this catalyst is not easily poisoned by CO, which increases the overall efficiency of ethanol oxidation making it more stable than other catalysts [46]. In addition, the low onset potential for this catalyst, namely -0.213 V, indicates that the ethanol electrooxidation reaction starts at a lower potential so that the reaction can occur with less energy [47].

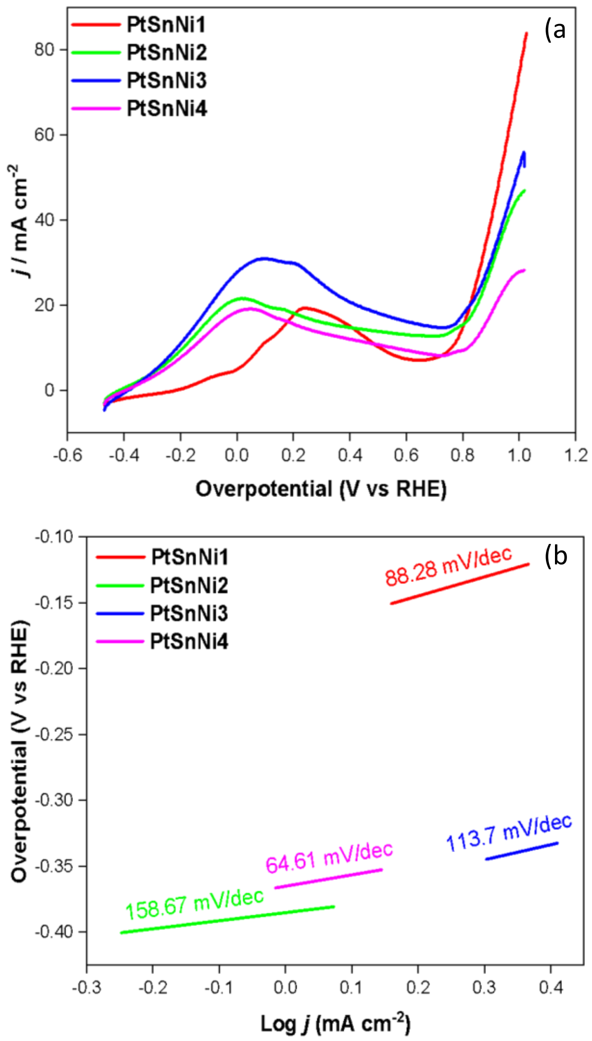

Figure 4. (a) LSV curves of PtSnNi and related (b) Tafel slope of experimental under 1.0 M ethanol and 1.0 M NaOH.

The EIS results further support the CV test findings, showing that the PtSnNi2 catalyst has the lowest R_{ct} value. A low R_{ct} indicates efficient and rapid electron transfer between ethanol molecules and the catalyst [48]. These findings align with SEM data, which confirm that the morphology and particle size of the PtSnNi2 catalyst are superior to those of other catalysts, resulting in the best catalytic activity and stability.

The PtSnNi2 catalyst has the smallest and most uniform particle size compared to other PtSnNi catalysts, which is closely related to the amount of current produced. The smaller and more uniform the particles, the greater the number of active sites available for the ethanol electrooxidation process. Additionally, PtSnNi2 catalysts have a spherical shape and lack agglomeration, as agglomeration can reduce their catalytic activity [49].

In contrast, the PtSnNi1 catalyst exhibits a less ideal morphology, with particles resembling ice flowers. This morphology promotes agglomeration, leading to a reduced active surface area and diminished reaction efficiency. The superiority of the $Pt_{73}Sn_{26}Ni_1$ catalyst over those with different compositions can be attributed to the optimal role and balance of its constituent elements.

The PtSnNi2 catalyst exhibited the best performance compared to other synthesized catalysts. Pt serves as the primary active element in the ethanol electrooxidation reaction. The relatively high Pt content in PtSnNi2, at 73%, ensures the availability of numerous active sites for ethanol oxidation. However, an excessively high Pt content, such as 90% and 93%, reduces activity due to insufficient Sn and Ni content, which limits the enhancement of reaction efficiency. Conversely, a very low Pt content, as in the catalyst with 13% Pt, results in too few active sites, thereby hindering efficient oxidation and reducing catalytic activity [50].

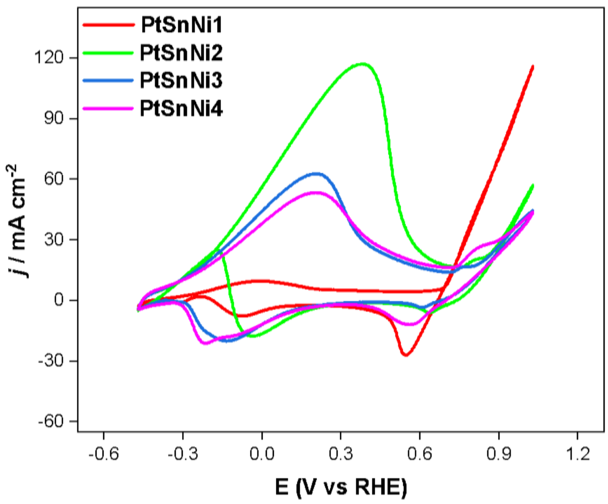

Figure 5. EOR test for all PtSnNi samples.

In addition to the active sites of Pt, Sn plays a critical role in preventing CO_{ads} poisoning by forming oxides that oxidize CO to CO_2 [51–53]. Low Sn contents, such as 4% and 8%, are ineffective at mitigating CO poisoning. On the other hand, an excessively high Sn content, such as 70 wt.% in PtSnNi1, decreases catalytic activity because Sn and its oxides have poor electronic conductivity, thereby lowering overall cell performance. The Ni element, present at 1 wt.% in PtSnNi2, contributes by breaking C-C bonds in the ethanol molecule, enhancing reaction efficiency. However, SEM results indicate that a high Ni content, such as 10% in PtSnNi1, leads to agglomeration, which reduces the active surface area and negatively impacts catalytic performance.

Table 4. Representation of EOR test in PtSnNi samples.

Sample	j (mA/cm^2)	Onset potential (V)	I_b/I_f
PtSnNi1	9.70	-0.283	0.7954
PtSnNi2	117.25	-0.213	0.1508
PtSnNi3	62.84	-0.238	0.3185
PtSnNi4	53.47	-0.243	0.3966

4. Conclusion

PtSnNi trimetallics were successfully synthesized using the electrodeposition method with various compositions. The PtSnNi2 sample, with Pt, Sn, and Ni compositions of 73 wt.%, 26 wt.%, and 1 wt.%, respectively, exhibited a spherical morphology with the smallest particle size and uniform distribution. The results of the EOR test demonstrated that PtSnNi2 generated a higher electric current compared to the sample with the highest Pt composition. This improvement is attributed to the synergistic effect between Pt, Sn, and Ni, which facilitates the oxidation of intermediate species, thereby enhancing the catalytic performance of the PtSnNi catalyst. These findings offer new trimetallic PtSnNi catalysts with high activities toward EOR and its stability. This study is crucial to the improvement of catalyst for EOR test in the future that can be further developed by manipulating the size and morphology.

Author contributions

Hilman Syafei: writing-original draft, investigation. Raudhatul Hadawiyah: writing-original draft & review, investigation. Mulya Muhammad Nur: Investigation, writing-review & editing.

Conflict of interest

There are no conflicts to declare

Acknowledgement

The authors thank the Lembaga Pengelola Dana Pendidikan (LPDP) Ministry of Finance, Republic of Indonesia, through Riset dan Inovasi Untuk Indonesia Maju (RIIM).

References

[1] P.K. Ozili, E. Ozen, Global Energy Crisis, *Impact Clim. Chang. Sustain. Stand. Insur. Mark.* (2023) 439–454. https://doi.org/10.1002/9781394167944.ch29.

[2] J. Wang, W. Azam, Natural resource scarcity, fossil fuel energy consumption, and total greenhouse gas emissions in top emitting countries, *Geosci. Front.* **15** (2024) 101757. https://doi.org/10.1016/j.gsf.2023.101757.

[3] P. Dos Santos Correa, E.L. Da Silva, S.C. De Sa, C. Radtke, E.S. Rieder, C.D.F. Malfatti, Catalyst based on Pt, Sn and Ni: Effect of carbon functionalization on ethanol electro-oxidation, *Proc. IEEE Conf. Nanotechnol.* (2012). https://doi.org/10.1109/NANO.2012.6322233.

[4] W. Ye, J. Yan, Q. Ye, F. Zhou, Template-free and direct electrochemical deposition of hierarchical dendritic gold microstructures: Growth and their multiple applications, *J. Phys. Chem. C*. **114** (2010) 15617–15624. https://doi.org/10.1021/jp105929b.

[5] Z.L. Liu, R. Huang, Y.J. Deng, D.H. Chen, L. Huang, Y.R. Cai, Q. Wang, S.P. Chen, S.G. Sun, Catalyst of Pt nanoparticles loaded on multi-walled carbon nanotubes with high activity prepared by electrodeposition without supporting electrolyte, *Electrochim. Acta*. **112** (2013) 919–926. https://doi.org/10.1016/j.electacta.2013.05.139.

[6] T.S. Almeida, A.R. Van Wassen, R.B. Vandover, A.R. De Andrade, H.D. Abruña, Combinatorial PtSnM (M = Fe, Ni, Ru and Pd) nanoparticle catalyst library toward ethanol electrooxidation, *J. Power Sources*. **284** (2015) 623–630. https://doi.org/10.1016/j.jpowsour.2015.03.055.

[7] C. Sun, H. Zhang, H. Liu, X. Zheng, W. Zou, L. Dong, L. Qi, Enhanced activity of visible-light photocatalytic H2 evolution of sulfur-doped g-C3N4 photocatalyst via nanoparticle metal Ni as cocatalyst, *Appl. Catal. B Environ.* **235** (2018) 66–74. https://doi.org/10.1016/J.APCATB.2018.04.050.

[8] S. Li, Y. Wang, S. Peng, L. Zhang, A.M. Al-Enizi, H. Zhang, X. Sun, G. Zheng, Co-Ni-Based Nanotubes/Nanosheets as Efficient Water Splitting Electrocatalysts, *Adv. Energy Mater.* **6** (2016) 1–7. https://doi.org/10.1002/aenm.201501661.

[9] X. Yin, Q. Liu, Y. Yang, Y. Liu, K. Wang, Y. Li, D. Li, X. Qiu, W. Li, J. Li, An efficient tandem photoelectrochemical cell composed of FeOOH/TiO 2 /BiVO 4 and Cu 2 O for self-driven solar water splitting, *Int. J. Hydrogen Energy*. **44** (2019) 594–604. https://doi.org/10.1016/j.ijhydene.2018.11.032.

[10] N.S.A. Malek, Y. Mohd, EFFECT OF DEPOSITION TIME ON STRUCTURAL AND CATALYTIC PROPERTIES OF Pt FILMS ELECTRODEPOSITED ON Ti SUBSTRATE, *Malaysian J. Anal. Sci.* **23** (2019) 52–59.

[11] A. Ourari, R. Zerdoumi, R.-R. Ramiro, E. Murallon,

Synthesis and Catalytic Properties of Modified Electrodes by Pulsed Electrodeposition of Pt/PANI Nanocomposite, *Materials (Basel).* **12** (2019). https://doi.org/10.3390/ma12050723.

[12] J. Friedl, U. Stimming, Model catalyst studies on hydrogen and ethanol oxidation for fuel cells, *Electrochim. Acta*. **101** (2013) 41–58. https://doi.org/10.1016/j.electacta.2012.12.130.

[13] S.P.S. Badwal, S. Giddey, A. Kulkarni, J. Goel, S. Basu, Direct ethanol fuel cells for transport and stationary applications - A comprehensive review, *Appl. Energy*. **145** (2015) 80–103. https://doi.org/10.1016/j.apenergy.2015.02.002.

[14] C. Bianchini, P.K. Shen, Palladium-based electrocatalysts for alcohol oxidation in half cells and in direct alcohol fuel cells, *Chem. Rev.* **109** (2009) 4183–4206. https://doi.org/10.1021/cr9000995.

[15] L. An, T.S. Zhao, Y.S. Li, Carbon-neutral sustainable energy technology: Direct ethanol fuel cells, *Renew. Sustain. Energy Rev.* **50** (2015) 1462–1468. https://doi.org/10.1016/j.rser.2015.05.074.

[16] A.Y. Kudhur, E.T. Salim, I. Kara, R.O. Mahdi, F.H. Alsultany, Applications of Cu2O Nanoparticles Prepared via Various Techniques: A Review Paper, *International Journal of Nanoelectronics and Materials*,**15** (2022) 131-137.

[17] S.P. Babu, P. Elumalai, Ethanol electrooxidation in alkaline medium on electrochemically synthesized Co(OH)2/Au composite, *Mater. Res. Express*. **4** (2017). https://doi.org/10.1088/2053-1591/aa5665.

[18] D.I. Syafei, H. Syafei, Square-Wave Pulse Deposition of Pt Nanoparticles for Ethanol Electrooxidation, *Chem. Mater.* **3** (2024) 21–26. https://doi.org/10.56425/cma.v3i1.70.

[19] C.V.S. Almeida, K.I.B. Eguiluz, G.R. Salazar-Banda, Superior ethanol electrooxidation activity of Pd supported on Ni(OH)2/C. The effect of Ni(OH)2 nanosheets content, *J. Electroanal. Chem.* **878** (2020). https://doi.org/10.1016/j.jelechem.2020.114683.

[20] M. Braun, M. Chatwani, P. Kumar, Y. Hao, I. Sanjuán, A.A. Apostoleri, A.C. Brix, D.M. Morales, U. Hagemann, M. Heidelmann, J. Masa, W. Schuhmann, C. Andronescu, Cobalt nickel boride as electrocatalyst for the oxidation of alcohols in alkaline media, *JPhys Energy*. **5** (2023). https://doi.org/10.1088/2515-7655/acbb2a.

[21] A.A. Maizelis, Electrooxidation of ethanol on nickel-copper multilayer metal hydroxide electrode, *Springer Proc. Phys.* **221** (2019) 59–68. https://doi.org/10.1007/978-3-030-17759-1_4.

[22] S.P. Nayak, L.K. Ventrapragada, S.S. Ramamurthy, J.K. Kiran Kumar, A.M. Rao, Green synthesis of a novel porous gold-curcumin nanocomposite for super-efficient alcohol oxidation, *Nano Energy*. **94** (2022). https://doi.org/10.1016/j.nanoen.2022.106966.

[23] M. Taei, E. Havakeshian, F. Abedi, M. Movahedi, The effect of Cu[sbnd]Mg[sbnd]Fe layered double hydroxide on the electrocatalytic activity of gold nanoparticles towards ethanol electrooxidation, *Int. J. Hydrogen Energy*. **41** (2016) 13575–13582. https://doi.org/10.1016/j.ijhydene.2016.06.229.

[24] M. Tran, C. Mundt, T. Lan, S. Padalkar, Electrodeposition of Gold Nanostructures Having Controlled Morphology, *J. Nanosci. Nanotechnol.* **18** (2017) 3492–3498. https://doi.org/10.1166/jnn.2018.14633.

[25] G. Yang, Q. Zhang, H. Yu, F. Peng, Platinum-based ternary catalysts for the electrooxidation of ethanol, *Particuology*. **58** (2021) 169–186. https://doi.org/10.1016/j.partic.2021.01.007.

[26] F. Xiao, Z. Mo, F. Zhao, B. Zeng, Ultrasonic-electrodeposition of gold-platinum alloy nanoparticles on multi-walled carbon nanotubes - ionic liquid composite film and their electrocatalysis towards the oxidation of nitrite, *Electrochem. Commun.* **10** (2008) 1740–1743. https://doi.org/10.1016/j.elecom.2008.09.004.

[27] M.A. García-Contreras, S.M. Fernández-Valverde, J.R. Vargas-García, Pt, PtNi and PtCoNi film electrocatalysts prepared by chemical vapor deposition for the oxygen reduction reaction in 0.5 M KOH, *J. Alloys Compd.* **504** (2010). https://doi.org/10.1016/j.jallcom.2010.03.206.

[28] B. Fang, PtCo-NC catalyst derived from the pyrolysis of Pt-incorporated ZIF-67 for alcohols fuel electrooxidation, *Wuli Huaxue Xuebao/ Acta Phys. -Chim. Sin.* **36** (2020). https://doi.org/10.3866/PKU.WHXB201905023.

[29] D.S.B.L. Oliveira, F. Colmati, E.R. Gonzalez, R. de Sousa Junior, Neurofuzzy modelling on the influence of Pt–Sn catalyst properties in direct ethanol fuel cells performance: Fuzzy inference system generation and cell power density optimization, *Int. J. Hydrogen Energy*. **48** (2023) 24481–24491. https://doi.org/10.1016/j.ijhydene.2023.03.137.

[30] A. Bonesi, G. Garaventa, W.E. Triaca, A.M. Castro

Luna, Synthesis and characterization of new electrocatalysts for ethanol oxidation, *Int. J. Hydrogen Energy*. **33** (2008) 3499–3501. https://doi.org/10.1016/j.ijhydene.2007.12.056.

[31] Y. Sun, H. Xiang, H. Li, G. Yu, H. Chen, S. Liu, High stability three-dimensional porous PtSn nano-catalyst for ethanol electro-oxidation reaction, *Chinese Chem. Lett.* **31** (2020) 2491–2494. https://doi.org/10.1016/j.cclet.2020.04.025.

[32] H. Luo, V.Y. Yukuhiro, P.S. Fernández, J. Feng, P. Thompson, R.R. Rao, R. Cai, S. Favero, S.J. Haigh, J.R. Durrant, I.E.L. Stephens, M.M. Titirici, Role of Ni in PtNi Bimetallic Electrocatalysts for Hydrogen and Value-Added Chemicals Coproduction via Glycerol Electrooxidation, *ACS Catal.* **12** (2022) 14492–14506. https://doi.org/10.1021/acscatal.2c03907.

[33] D.K. Mauer, S. V. Belenov, L.M. Skibina, V.E. Guterman, Composite Pt/(SnO2/C) and PtSnNi/C Catalysts for Oxygen Reduction and Alcohol Electrooxidation Reactions, *Russ. J. Electrochem.* **57** (2021) 898–910. https://doi.org/10.1134/S1023193521060069.

[34] T.S. Almeida, L.M. Palma, C. Morais, K.B. Kokoh, A.R. De Andrade, Effect of Adding a Third Metal to Carbon-Supported PtSn-Based Nanocatalysts for Direct Ethanol Fuel Cell in Acidic Medium, *J. Electrochem. Soc.* **160** (2013) F965–F971. https://doi.org/10.1149/2.025309jes.

[35] J. Asgardi, J.C. Calderón, F. Alcaide, A. Querejeta, L. Calvillo, M.J. Lázaro, G. García, E. Pastor, Carbon monoxide and ethanol oxidation on PtSn supported catalysts: Effect of the nature of the carbon support and Pt:Sn composition, *Appl. Catal. B Environ.* **168–169** (2015) 33–41. https://doi.org/10.1016/j.apcatb.2014.12.003.

[36] H. Syafei, Dwi Giwang Kurniawan, Electrodeposition of CoxNiy Thin Film and Its Catalytic Activity for Ethanol Electrooxidation, *Chem. Mater.* **2** (2023) 14–18. https://doi.org/10.56425/cma.v2i1.50.

[37] L. Jiang, A. Hsu, D. Chu, R. Chen, Ethanol electro-oxidation on Pt/C and PtSn/C catalysts in alkaline and acid solutions, *Int. J. Hydrogen Energy*. **35** (2010) 365–372. https://doi.org/10.1016/j.ijhydene.2009.10.058.

[38] F. Cao, Z. Zang, S. Sun, X. Sun, X. Li, T. Liu, J. Wu, The influence of deposited potential on the ORR activity of Pt catalysts on glassy carbon electrode, *RSC Adv.* **7** (2017) 25429–25436. https://doi.org/10.1039/c7ra02444d.

[39] Y. Lykhach, A. Figueroba, T. Skála, T. Duchoň, N. Tsud, M. Aulická, A. Neitzel, K. Veltruská, K.C. Prince, V. Matolín, K.M. Neyman, J. Libuda, Redox-mediated conversion of atomically dispersed platinum to sub-nanometer particles, *J. Mater. Chem. A*. **5** (2017) 9250–9261. https://doi.org/10.1039/c7ta02204b.

[40] A. Raveendran, M. Chandran, R. Dhanusuraman, A comprehensive review on the electrochemical parameters and recent material development of electrochemical water splitting electrocatalysts, *RSC Adv.* **13** (2023) 3843–3876. https://doi.org/10.1039/d2ra07642j.

[41] O. van der Heijden, S. Park, R.E. Vos, J.J.J. Eggebeen, M.T.M. Koper, Tafel Slope Plot as a Tool to Analyze Electrocatalytic Reactions, *ACS Energy Lett.* **9** (2024) 1871–1879. https://doi.org/10.1021/acsenergylett.4c00266.

[42] C. Lo Vecchio, E. Mosca, S. Trocino, V. Baglio, Investigation of an Ethanol Electroreforming Cell Based on a Pt1Ru1/C Catalyst at the Anode, *Catalysts*. **14** (2024) 415. https://doi.org/10.3390/catal14070415.

[43] J. Zhang, Cyclic Penta-Twinned Rhodium Nanobranches as Superior Catalysts for Ethanol Electro-oxidation, *J. Am. Chem. Soc.* **140** (2018) 11232–11240. https://doi.org/10.1021/jacs.8b03080.

[44] T.H. Huang, D. Bhalothia, S. Lin, Y.R. Huang, K.W. Wang, The ethanol oxidation reaction performance of carbon-supported PtRuRh nanorods, *Appl. Sci.* **10** (2020) 1–12. https://doi.org/10.3390/app10113923.

[45] F.Q. Shao, J.J. Feng, Z.Z. Yang, S.S. Chen, J. Yuan, A.J. Wang, Cytosine assisted aqueous synthesis of AgPt hollow alloyed nanostructures as highly active electrocatalyst for ethylene glycol oxidation and hydrogen evolution, *Int. J. Hydrogen Energy*. **42** (2017) 24767–24775. https://doi.org/10.1016/j.ijhydene.2017.08.078.

[46] D.H. Kwak, Y.W. Lee, S.B. Han, E.T. Hwang, H.C. Park, M.C. Kim, K.W. Park, Ultrasmall PtSn alloy catalyst for ethanol electro-oxidation reaction, *J. Power Sources*. **275** (2015) 557–562. https://doi.org/10.1016/j.jpowsour.2014.11.050.

[47] T.S. Almeida, K.B. Kokoh, A.R. De Andrade, Effect of Ni on Pt/C and PtSn/C prepared by the Pechini method, *Int. J. Hydrogen Energy*. **36** (2011) 3803–3810. https://doi.org/10.1016/j.ijhydene.2010.12.066.

[48] A.R. Bonesi, M.S. Moreno, W.E. Triaca, A.M.C. Luna,

Modified catalytic materials for ethanol oxidation, *Int. J. Hydrogen Energy*. **35** (2010) 5999–6004. https://doi.org/10.1016/j.ijhydene.2009.12.093.

[49] H.B. Hassan, Z.A. Hamid, R.M. El-Sherif, Electrooxidation of methanol and ethanol on carbon electrodeposited Ni-MgO nanocomposite, *Cuihua Xuebao/Chinese J. Catal.* **37** (2016) 616–627. https://doi.org/10.1016/S1872-2067(15)61034-8.

[50] D.S. Santos, C.V.S. Almeida, G. Tremiliosi-Filho, K.I.B. Eguiluz, G.R. Salazar-Banda, Improved carbon dioxide selectivity during ethanol electrooxidation in acid media by Pb@Pt/C and Pb@PtSn/C electrocatalysts, *J. Electroanal. Chem.* **879** (2020) 114741. https://doi.org/10.1016/j.jelechem.2020.114741.

[51] R.M.C. Silva, G.A. Camara, M.J. Giz, Electro-oxidation of ethanol on PtRh surfaces partially covered by Sn, *Electrochim. Acta*. **308** (2019) 167–173. https://doi.org/10.1016/j.electacta.2019.04.028.

[52] M. Roca-Ayats, G. Garcia, M. Soler-Vicedo, E. Pastor, M.J. Lazaro, M. V. Martinez-Huerta, The role of Sn, Ru and Ir on the ethanol electrooxidation on Pt3M/TiCN electrocatalysts, *Int. J. Hydrogen Energy*. **40** (2015) 14519–14528. https://doi.org/10.1016/j.ijhydene.2015.05.175.

[53] Q.N. Salsabila, F.G. Kenaya, M.F. Aulia, M. Athariq,Additive-free Electrodeposition of SnCoNi Trimetallic Catalysts for Ethanol Electrooxidation, *Chem. Mater.* **3** (2024) 90–97. https://doi.org/http://doi.org/10.56425/cma.v3i3.84.